RAPID COMMUNICATIONS

PHYSICAL REVIEW C VOLUME 48, NUMBER 2 AUGUST 1993

Widths of transverse momentum distributions in intermediate-energy heavy-ion collisions

Ferdous Khan
Physics Department, Old Dominion University, Norfolk, Virginia 23529

Lawrence W. Townsend
Mail Stop 493, NASA Langley Research Center, Hampton, Virginia 23681

(Received 9 April 1993)

The need to include dynamical collision momentum transfer contributions, arising from interacting nuclear and Coulomb fields, to estimates of fragment momentum distributions is discussed. Methods based upon an optical potential model are presented. Comparisons with recent experimental data of the Siegen group for variances of transverse momentum distributions for gold nuclei at 980A MeV fragmenting on silver foil and plastic nuclear track detector targets are made. The agreement between theory and experiment is good.

PACS number(s): 25.70.−z

Recently, Dreute *et al.* [1] reported measurements of fragment yields and transverse momentum distributions produced in the breakup of gold projectile nuclei with kinetic energies between 200A and 980A MeV. In their analyses of the data for transverse momentum distributions of light and heavy fragments, they found that the standard deviations σ (i.e., the so-called widths) of the distributions were considerably larger than those predicted by statistical models [2,3]. More recently, Morrissey [4] questioned these findings on the basis that the assumption of the same A/Z (mass-to-charge) ratio for the fragments as for the initial projectile could result in an overestimation of the heavy fragment transverse momentum distribution. Morrissey suggested that a better prescription for the fragment A/Z ratio is the one due to Sümmerer *et al.* [5], which favors more neutron-deficient fragments than are indicated by the A/Z ratio of the projectile. Following Morrissey's suggestion, Dreute *et al.* reanalyzed their data using the Sümmerer parametrization and concluded that the widths of the transverse momentum distributions were still significantly larger than statistical model predictions [6]. Application of the estimated charge-to-mass ratios from the gold spallation experiments of Cummings *et al.* [7] indicated that the fragments were even more neutron deficient than the Sümmerer *et al.* predictions and also indicated that the widths were still larger than those predicted by statistical models.

In earlier work, Brady *et al.* [8] measured similarly large values of transverse momentum widths of fragments produced by the breakup of 1.2A GeV lanthanum ions on carbon targets. Again, the analyses were performed using the assumption that the fragment A/Z ratio was that of the incident lanthanum nucleus. Based on the analyses by Dreute *et al.*, one suspects that these larger momentum widths will survive even if Brady *et al.* reanalyze their data using alternative A/Z prescriptions. Further evidence of the inadequacy of a purely statistical model in describing transverse momentum widths comes from the ^{84}Kr+^{197}Au reaction [9], target fragmentation data [10], other experiments by the Siegen group with lighter projectiles [11], the argon fragmentation measurements of Tull [12], and ^{16}O data at lower bombarding energies [13]. Recent experiments by Brady and collaborators [14] for Nb+C, La+C, and Au+C reactions again follow the same trend, i.e., the widths of the transverse momentum components of the fragments are significantly broader than predictions based upon momentum conservation and internal Fermi motion alone.

The solution to this quandary, as discussed in Refs. [2,15], lies in the dynamics of the collisional momentum transfers. Years ago, Goldhaber pointed out [Eq. (10) of Ref. [2]] that collision momentum transfers will modify the width of the momentum distribution in the direction of the momentum transfer according to

$$\sigma_i'^2=\sigma_i^2+\frac{F^2}{A^2}P_i^2 , \tag{1}$$

where $\sigma_i'^2$ is the modified width, P_i^2 is the mean squared momentum transfer in the ith component direction ($i=x,y,z$ in a Cartesian frame), A is the mass number of the fragmenting nucleus, F is the fragment mass number, and σ_i^2 is given by

$$\sigma_i^2=\sigma_0^2F(A-F)/(A-1) . \tag{2}$$

The parameter σ_0 is usually related to the Fermi momentum of the projectile (P_F) via

$$\sigma_0^2=P_F^2/5 , \tag{3}$$

where P_F is obtained from electron-scattering measurements. Since no simple, well-defined prescription existed for estimating collision momentum transfers, it became customary to write

$$\sigma_i'^2=\sigma_{0,\mathrm{exp}}^2F(A-F)/(A-1) , \tag{4}$$

where the $\sigma_{0,\mathrm{exp}}^2$ are deduced from the experimental measurements of $\sigma_i'^2$ and then directly compared with σ_0^2 obtained from Eqs. (2) and (3). For example, in their pioneering measurements at the Bevalac, Greiner and collaborators [16] reported that the fitted values of σ_0 ob-

tained from Eq. (4) were about 10–20 percent smaller than those based upon measured Fermi momenta (from electron-scattering data) for the breakup of the light nuclei ^{12}C and ^{16}O projectiles at energies above $1A$ GeV. The experimental and theoretical situations up to 1984 have been described in detail by Stokstad [17].

In recent work [15], an optical model momentum transfer formalism was developed and used to successfully describe the measured momentum distributions of ^{139}La fragmentations at high energies [8]. In Ref. [15] it is shown that the transverse component of the momentum transfer can be estimated from

$$\mathbf{Q}_\perp(E,b) = -A_P A_T \int d^3\xi_P \rho_P(\xi_P) \int d^3\xi_T \rho_T(\xi_T) \nabla_P \int_{-\infty}^{\infty} \mathrm{Re}\tilde{t}(E, \mathbf{b}+\mathbf{z}'+\boldsymbol{\xi}_P-\boldsymbol{\xi}_T) \frac{dz'}{v} \ . \tag{5}$$

In Eq. (5) the collision momentum transfer for each projectile nucleon-target nucleon pair is given by the gradient of the nucleon-nucleon (NN) t matrix. This results in an NN momentum transfer which is a function of the NN separation ($\mathbf{y}=\mathbf{b}+\mathbf{z}'+\boldsymbol{\xi}_P-\boldsymbol{\xi}_T$). To obtain the total momentum transfer in the nucleus-nucleus collision, we integrate over the projectile and target nuclear density distributions. The integration along the beam direction z' arises from the usual time integration ($dt=dz'/v$) associated with the collision impulse. In Eq. (5) the nuclear densities ρ_i ($i=P,T$) are normalized to unity, the A_i are the mass numbers of the colliding nuclei, and v is their relative velocity. The gradient is taken with respect to the projectile internal coordinates $\boldsymbol{\xi}_P$ and $\tilde{t}$ is the complex, constituent-averaged, two-nucleon transition amplitude. The latter is the Fourier transform of the elastic scattering amplitude and is parametrized in the usual way [18] as

$$\tilde{t}(E,\mathbf{x}) = -(E/m)^{1/2}\sigma(E)[\alpha(E)+i][2\pi B(E)]^{-3/2} \times \exp[-x^2/2B(E)] \ , \tag{6}$$

where E is the two-nucleon kinetic energy in their center-of-mass frame, $\sigma(E)$ is the nucleon-nucleon total cross section, $\alpha(E)$ is the ratio of the real-to-imaginary part of the forward scattering amplitude, and $B(E)$ is the nucleon-nucleon slope parameter (which describes the decrease in the NN differential cross section as the momentum transfer increases). Values for these parameters are taken from various compilation and are listed in Ref. [19].

At energies $\leq 400A$ MeV, nonlocal effects and other modifications of the nucleon-nucleon interaction are important. Also, compression effects lead to higher densities of the system. To account for these effects, the total transverse momentum per nucleon is defined to be [20]

$$\mathbf{P}_\perp(E,b)/A = [\mathbf{Q}_\perp(E,b) - \mathbf{Q}_\perp(E_0,b)]/A \ , \tag{7}$$

where E_0 is the balance energy (in MeV per nucleon) for the system. The values of E_0 used to evaluate Eq. (7) were taken from balance energy systematics [21]. For Au+Ag collisions, $E_0=47A$ MeV, and for Au+C (C is a major CR-39 constituent) collisions, $E_0=50A$ MeV. Note that all of the energy dependence in Eq. (7) arises from the energy dependence in the transition amplitude [Eq. (6)].

When evaluating Eq. (7), free-space, two-body transition amplitudes are used at the beam energy of $980A$ MeV to compute $Q_\perp(E,b)$. To compute the balance-energy correction [$Q_\perp(E_0,b)$], however, free-space amplitudes are found to be inadequate. This is not surprising since it is well known that medium effects significantly modify the free nucleon-nucleon interaction at these lower energies (e.g., $\sim 50A$ MeV). Therefore, the slope parameter $B(E)$ and nucleon-nucleon cross section $\sigma(E)$ may be significantly different, in low- and intermediate-energy nucleus-nucleus collisions, from their free-space, two-nucleon values. To modify these, we note that in the nuclear medium the local mean free path λ is significantly larger [22] than the value obtained from

$$\lambda = (\rho_0 \sigma_{NN})^{-1} \ , \tag{8}$$

where σ_{NN} is the usual free-space nucleon-nucleon total cross section, and $\rho_0=0.17$ fm^{-3} is the nuclear number density. This increase in the mean-free path arises from Pauli blocking of intermediate states and nonlocal effects. Although Eq. (7) is written to account for nonlocal effects, it does not properly account for the effects of Pauli blocking. One method to account for this is to use medium-modified cross sections $\tilde{\sigma}_{NN}(E)$ and slope parameters $\tilde{B}(E)$ in the transition amplitude [Eq. (6)]. For the present work, we will focus only on $\tilde{\sigma}_{NN}(E)$ and assume that $\tilde{B}(E) \approx B(E)$.

A simple method for estimating $\tilde{\sigma}_{NN}$ is to use phenomenological mean-free paths obtained from experimental nucleon-nucleus cross-section measurements [23]. An accurate parametrization of these is given by [24]

$$\lambda = 16.6E^{-0.26} \ , \tag{9}$$

where λ is in units of fm, and E is the beam energy in MeV/nucleon. Note that mean-free-path values given by Eq. (9) are nearly identical to those derived from nonlocal, optical-model calculations [22]. At $E=50A$ MeV, Eq. (9) yields $\lambda=6$ fm. Inserting this into Eq. (8) and solving for the cross section yields $\tilde{\sigma}_{NN}=10.2$ mb. This value is used herein to calculate $Q_\perp(E_0,b)$ in Eq. (7).

One final input remains. Since $P_\perp(b)$ is a function of impact parameter, an appropriate method for choosing the most probable impact parameter for each fragmentation channel is necessary. As before [15], the most probable impact parameter for each nucleon removal channel ΔA (=1,2,3, etc.) is estimated using a semiempirical model. For this work, we use HZEFRG1 [24], a newly-developed model which incorporates the λ from Eq. (9) and actual nuclear charge radii from electron scattering into a geometric abrasion-ablation-frictional spectator interaction (FSI) formalism. These "most probable" im-

TABLE I. Most probable impact parameters (b, in fm) and x components of transverse momentum transfer (P_x in MeV/c) as a function of fragment mass number (F) for 980A MeV gold nuclei fragmenting on silver and carbon targets.

F	b	$P_x(b)$
	Silver target	
175	11.68	246
150	10.55	843
125	9.53	1700
100	8.60	2581
75	7.75	3377
50	6.95	4001
25	6.22	4474
	Carbon target	
195	10.00	23
175	8.71	158
150	7.27	550
125	5.91	879

pact parameters are inserted into Eqs. (5) and (7) to obtain the corresponding transverse momentum transfers $P_\perp(b)/A$. These are converted to x (or y) components using the assumption $P_x(b)=P_y(b)=P_\perp(b)/\sqrt{2}$ since no significant experimental differences were found for the x and y variances of the transverse momentum distributions in the experiments [1].

Table I displays representative values of the most probable impact parameters and $P_x(b)$ for various fragment masses F for 980A MeV ^{197}Au projectiles fragmenting on Ag and C targets. Figure 1 displays transverse momentum widths (dashed curves) obtained using these values of $P_x(b)$ in Eqs. (1) and (2) with $\sigma_0=112$ MeV/c (which corresponds to a Fermi momentum of $P_F\approx 250$ MeV/c). The agreement with the experimental data of Ref. [6] is satisfactory. In their work, Brady *et al.* [8] suggested that Coulomb repulsion could play a significant role in determining fragment momentum widths. To investigate this possibility, we add a Coulomb contribution in quadrature to Eq. (1) as

$$\sigma_i'^2=\sigma_i^2+\frac{F^2}{A^2}P_i^2+\frac{F^2}{A^2}P_{i,c}^2 , \tag{10}$$

where $P_{i,c}$ is the ith component of the Coulomb contribution to the momentum transfer. It is calculated using Eq. (13.1) of Ref. [25]. The resultant Coulomb-modified widths are represented in Fig. 1 as the solid curves. Note that, as expected, there is a slight increase in the estimated values for σ'. The agreement between theory and experiment is still good. Improved agreement might be obtained with a more sophisticated treatment of the Coulomb repulsion. Nevertheless, the present agreement is satisfactory for demonstrating the inadequacies of the statistical model and for demonstrating the essential need to incorporate collisional momentum transfer contributions into any realistic description of these phenomena. Our multiple-scattering-theory-based approach provides a convenient analytical tool for investigating heavy ion momentum transfers and the associated fragment momentum distributions.

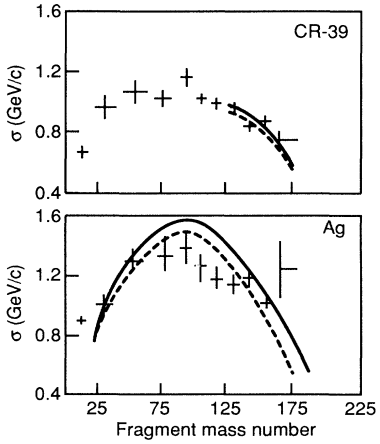

FIG. 1. Standard deviations σ of transverse momentum distributions for 980A MeV gold nuclei fragmenting on Ag foil and plastic nuclear track detector (CR-39) targets. The experimental data (crosses), for $M=1$ multiplicity fragments, were taken from Ref. [6]. The calculated values, obtained using the methods discussed in the text, were estimated for Ag and C (a major constituent of CR-39) targets. The solid curve includes Coulomb effects, and the dashed curve does not.

One of the authors (F.K.) gratefully acknowledges research support from the National Aeronautics and Space Administration.

[1] J. Dreute, W. Heinrich, G. Rusch, and B. Wiegel, Phys. Rev. C **44**, 1057 (1991).
[2] A. S. Goldhaber, Phys. Lett. **53B**, 306 (1974).
[3] D. J. Morrissey, Phys. Rev. C **39**, 460 (1989).
[4] D. J. Morrissey, Phys. Rev. C **47**, 413 (1993).
[5] K. Sümmerer, W. Brüchle, D. J. Morrissey, M. Schädel, B. Szweryn, and Yang Weifan, Phys. Rev. C **42**, 2546 (1990).
[6] J. Dreute, W. Heinrich, G. Rusch, and B. Wiegel, Phys. Rev. C **47**, 415 (1993).
[7] J. R. Cummings, W. R. Binns, T. L. Garrard, M. H. Israel, J. Klarmann, E. C. Stone, and C. J. Waddington, Phys. Rev. C **42**, 1508 (1990).
[8] F. P. Brady *et al.*, Phys. Rev. Lett. **60**, 1699 (1988).
[9] C. Stephan *et al.*, Phys. Lett. B **262**, 6 (1991).
[10] D. J. Morrissey, Phys. Rev. C **39**, 460 (1989).
[11] H. Drechsel, C. Brechtmann, W. Heinrich, and J. Dreute, Phys. Rev. Lett. **55**, 1258 (1983).
[12] C. E. Tull, Ph.D. thesis, University of California–Davis, Lawrence Berkeley Laboratory Report No. LBL-29718, 1990.
[13] K. VanBibber *et al.*, Phys. Rev. Lett. **42**, 33 (1979).
[14] F. P. Brady *et al.*, unpublished; F. P. Brady, private communication.
[15] F. Khan, G. S. Khandelwal, L. W. Townsend, J. W. Wilson, and J. W. Norbury, Phys. Rev. C **43**, 1372 (1991).

[16] D. E. Greiner, P. J. Lindstrom, H. H. Heckman, B. Cork, and F. S. Bieser, Phys. Rev. Lett. **35**, 152 (1975).
[17] R. G. Stokstad, Comments Nucl. Part. Phys. **13**, 231 (1984).
[18] V. Franco, Phys. Rev. Lett. **32**, 911 (1974).
[19] L. W. Townsend and J. W. Wilson, NASA Reference Publication No. RP-1134, 1985.
[20] F. Khan, L. W. Townsend, R. K. Tripathi, and F. A. Cucinotta, Phys. Rev. C **48**, 926 (1993).
[21] R. K. Tripathi, L. W. Townsend, and F. Khan, Phys. Rev. C **47**, R935 (1993).
[22] J. W. Negele and K. Yazaki, Phys. Rev. Lett. **47**, 71 (1981).
[23] R. Dymarz and T. Kohmura, Oxford University Report No. 58/82, 1982.
[24] L. W. Townsend, J. W. Wilson, R. K. Tripathi, J. W. Norbury, F. F. Badavi, and F. Khan, NASA Technical Paper No. TP-3310, 1993.
[25] J. D. Jackson, *Classical Electrodynamics,* 2nd Ed. (Wiley, New York, 1975), Chap. 13.